*33rd EPS Conference on Plasma Phys. Rome, 19 - 23 June 2006 ECA Vol.**30I**, P-1.080 (2006)*

Modelling of effects of ripple-induced thermal ion losses on JET and JT-60U H-mode plasmas

J.-S. Lönnroth[1], V. Parail[2], T. Johnson[3], T. Kiviniemi[1], N. Oyama[4], G. Saibene[5], P. de Vries[2], T. Hatae[4], V. Hynönen[1], Y. Kamada[4], S. Konovalov[4], A. Loarte[5], A. Salmi[1], K. Shinohara[4], K. Tobita[4], H. Urano[4] and JET EFDA contributors*

[1]*Association EURATOM-Tekes, Helsinki University of Technology, Finland*
[2]*EURATOM/UKAEA Fusion Association, Culham Science Centre, United Kingdom*
[3]*Association EURATOM-VR, Royal Institute of Technology, Stockholm, Sweden*
[4]*Japan Atomic Energy Agency, Naka, Ibaraki-ken, 311-0193, Japan*
[5]*EFDA Close Support Unit, c/o Max Planck Institut für Plasmaphysik, Garching, Germany*
**See Appendix of J.Paméla et al., Fusion Energy 2004 (Proc. 20th Int. Conf. Vilamoura) IAEA, Vienna (2004)*

Introduction

The discreteness of the toroidal magnetic field coil configuration in tokamaks shows up as ripple in the toroidal magnetic field, which results in ripple losses of both thermal and fast ions. The effects of ripple-induced fast ion losses have been investigated in several studies, both experimentally and theoretically, and on several machines [1, 2]. Perhaps due to associations with L-mode physics, ripple transport due to thermal ion losses has until recently been relatively unexplored. In the L-mode, all transport coefficients have relatively large values in the region just inside the separatrix, in comparison to which any ripple-induced additional transport is negligible. In the H-mode, on the other hand, transport within the edge transport barrier (ETB) is suppressed to a very low level, whereby the effects of any additional ripple-induced transport can be very discernible.

Recently, the results of a series of dimensionless pedestal identity experiments at JET and JT-60U have prompted speculation that the relatively large ripple amplitude at JT-60U could be one reason for the high ELM frequency and modest pedestal performance seen in many JT-60U plasmas. Despite a good match in all main dimensionless parameters (ρ*, β, ν*), the ELM frequency is generally lower and the pedestal performance better in the JET discharges than in their JT-60U matches[3]. MHD stability analysis does not explain this result, even if toroidal rotation and the explicit dependence on the aspect ratio are taken into account in the analysis. On the contrary, it has been shown that discharges from the two machines have very similar stability characteristics.

Orbit-following simulations

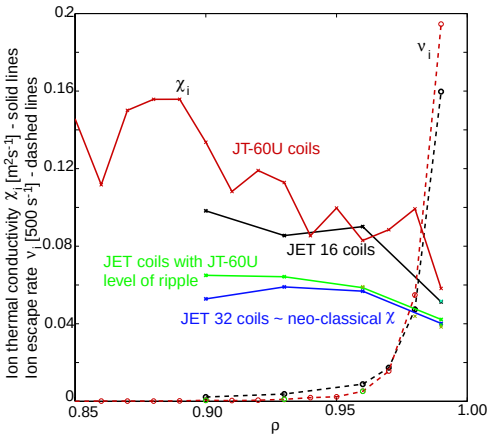

The effects of ripple losses of thermal ions on ion thermal transport have been studied in orbit-following simulations with the Monte Carlo orbit-following code ASCOT [4]. Figure 1 illustrates a characteristic result of the ASCOT simulations. Shown in the figure are radial profiles of the ion thermal conductivity induced by losses due to diffusive transport and of the ion escape rate due to non-diffusive (orbit) losses.

Figure 1. Collisional transport of thermal ions in JET discharge 60856 for a series of JET and JT-60U magnetic coil configurations as computed by ASCOT.

The first obvious conclusion from the figure is that the level of ripple-induced transport can be significant in comparison to the ion neo-classical level of transport within the ETB. Secondly, losses due to diffusive transport give rise to a broad radial profile of additional thermal conductivity, whereas non-diffusive losses are very edge-localized. Finally, the JT-60U configuration leads to a higher level of ripple-induced transport than the JET one.

Modelling of the effects of non-diffusive losses

The results of the orbit-following simulations have been applied in predictive transport modelling with the JETTO transport code. The so-called τ approximation was introduced, in which a convective energy sink term is included into the continuity equation for the ion pressure. ELMs have been modelled with a simple *ad hoc* model [5]. When a fixed critical pressure gradient is exceeded somewhere within the pedestal, all transport coefficients are increased to pre-defined levels for a pre-defined duration of time in this region.

Figure 2 illustrates some characteristic results obtained with the model for non-diffusive losses. Two simulations are used in each figure, one reference simulation with no losses and another one with a maximum loss rate of $\nu = 100\ s^{-1}$. In order to reflect the fact that non-diffusive losses are very edge-localized, the ion escape rate profile $\nu(\rho)$ has been kept zero throughout most of the core plasma and then ramped up linearly at the edge from $\rho = 0.90$, where ρ is the square root of the normalized toroidal flux. This is illustrated in frame (a) in Fig. 2, which shows $\nu(\rho)$ in the two simulations. Frame (b) in Fig. 2, which shows the pressure profiles in the two simulations at times shortly before ELMs, illustrates the effect on plasma performance. It can be seen that there is a flattening of the pressure profile just inside the separatrix in the simulation modelling non-diffusive losses, which results in an effective narrowing of the pedestal. This effective narrowing of the pedestal leads to a lower top-of-the-pedestal pressure, which due to profile stiffness translates into lower pressure throughout the core plasma and thus into reduced confinement The effect on the ELM frequency is illustrated in frame (c) in Fig. 2, which shows time traces of the ion thermal conductivity at the flux surface $\rho = 0.95$ as a function of time in the two simulations. The ELM frequency increases with increasing non-diffusive losses mainly because of profile stiffness, which leads to increased transport inside the pedestal in the case of lower pedestal height.

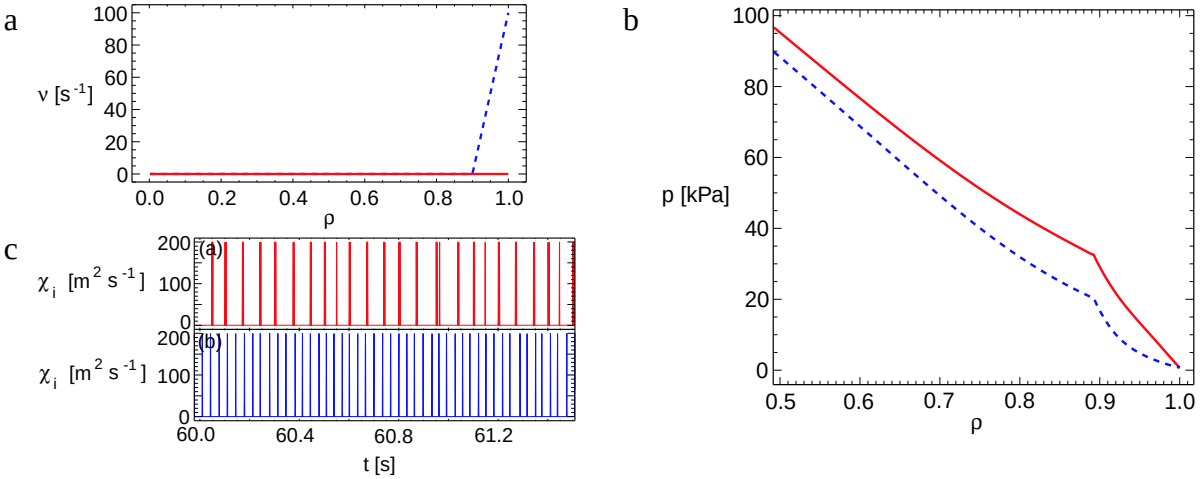

Figure 2. (a) Radial profiles of the imposed ion escape rate in a simulation with the τ approximation model for non-diffusive losses (dashed curve) and in a reference simulation with no imposed losses (solid curve). (b) Radial profiles of the total pressure. (c) Ion thermal conductivity at the magnetic surface $\rho = 0.95$ as a function of time.

The reduced plasma confinement and increased ELM frequency obtained in the simulations with non-diffusive losses resemble the results obtained at JT-60U in the pedestal identity ex-

periments. This implies that non-diffusive losses associated with the stronger magnetic ripple at JT-60U might explain the lower pedestal performance and higher ELM frequency in comparison to JET at this machine.

Modelling of the effects of losses due to diffusive transport

In modelling the effects of losses due to diffusive transport, a simple analytical approximation [6] for ripple-induced diffusive transport was introduced. In accordance with the ASCOT simulations, it was assumed that the ripple-induced ion thermal conductivity has a distribution with a characteristic width significantly wider than the pedestal width. Figure 3 illustrates a set of results from this study. The radial profile of the inter-ELM ion thermal conductivity used in the simulation is shown in frame (a) in Fig. 3 together with the profile from a reference simulation without additional transport. It should be noted that the transport perturbation is significant in amplitude well beyond the top of the pedestal in comparison with the ion neo-classical level of ion thermal conductivity within the ETB.

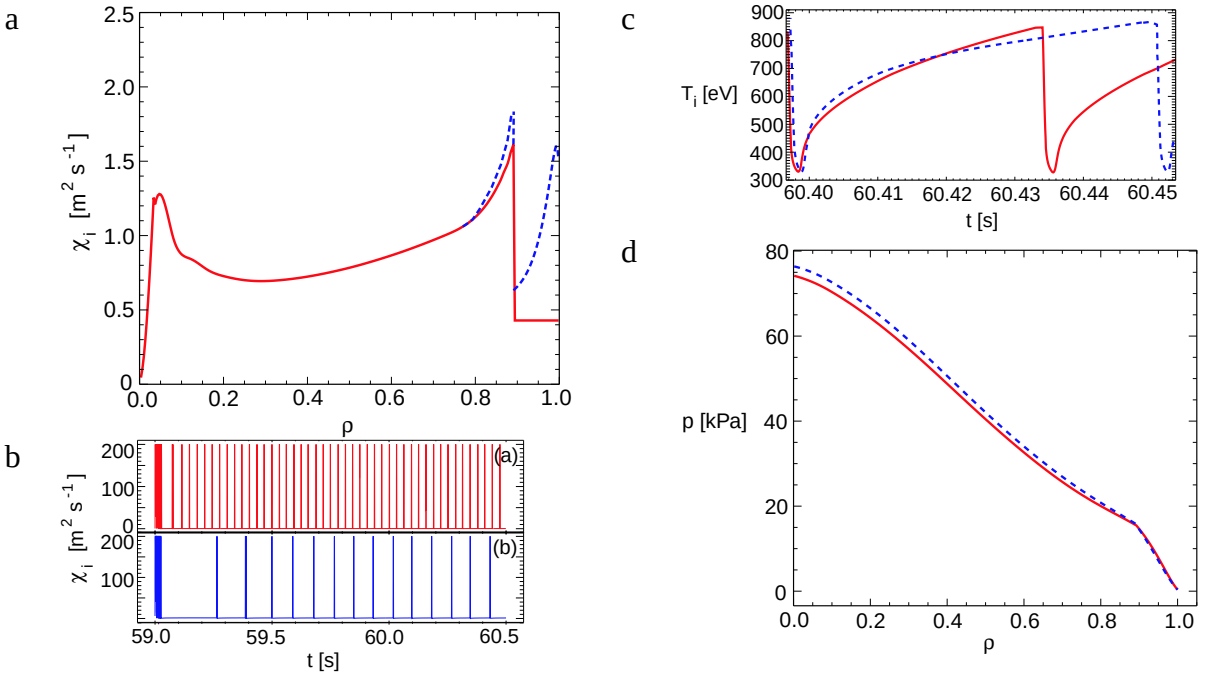

Figure 3. (a) Radial profiles of ion thermal conductivity in two predictive transport simulations without (solid curve) and with (dashed curve) a contribution representing ripple-induced ion thermal transport at the edge. (b) Ion thermal conductivity at the magnetic surface ρ = 0.95 as a function of time. (c) Ion temperature at the top of the pedestal as a function of time for the duration of the longer of the two ELM cycles. (d) Radial profiles of the total pressure at times shortly before ELMs.

The effect on the ELM frequency of introducing the transport perturbations can be seen in frame (b) in Fig. 3, which shows the ion thermal conductivity at ρ = 0.95 as a function of time. In this case, the ELM frequency decreases noticeably with the introduction of additional transport at the edge. The explanation for this is that the increased transport at the edge leads to increased losses between the ELMs and thus to a longer ELM build-up time.

As a result of the lower ELM frequency with the introduction of ripple-induced transport, the average top-of-the-pedestal temperature increases considerably, even though the ultimate pre-ELM pedestal height does not change. The time-average temperature at the top of the pedestal is larger for slower pedestal build-up, because the temperature generally increases most rapidly for a relatively constant amount of time right after an ELM crash and then saturates more and more slowly over time before the next ELM. This is illustrated in frame (c) in Fig.

3, which shows the ion temperature at the top of the pedestal as a function of time for the duration of the longer of the two ELM cycles in the simulations with and without ripple-induced transport. It is evident that the average of the electron and ion temperatures is higher in the case with lower ELM frequency

The effect on plasma performance becomes evident in frame (d) in Fig. 3, which shows the pressure profiles in the simulations at times shortly before ELMs. The maximum pressure at the top of the pedestal is the same in the two cases, but since the lower ELM frequency in the simulation with ripple-induced transport leads to higher average top-of-the-pedestal temperature and thus to higher average top-of-the-pedestal pressure, the core pressure becomes higher in this case thanks to profile stiffness. In this way, ripple-induced additional ion thermal transport at the edge can lead to improved overall confinement. It should be noted that the simulation results resemble the improved performance obtained with the introduction of a stochastic magnetic boundary layer in some DIII-D plasmas [7] and the slight improvement in confinement obtained with small ripple amplitudes in previous JET experiments[8].

Conclusions

The effects of ripple-induced thermal ion losses on H-mode plasmas have been studied. Orbit-following simulations show that both losses due to diffusive transport and non-diffusive losses can be important. Predictive transport modelling indicates that non-diffusive losses, which are very edge-localized, can lead to a deterioration of pedestal performance and an increase in the ELM frequency. This behaviour characteristically resembles the observations at JT-60U in dimensionless pedestal identity experiments with JET. Modelling of losses due to diffusive transport, which result in a broad radial profile of enhanced ion thermal conductivity, shows that ripple losses need not necessarily have a detrimental influence on plasma performance. On the contrary, the results suggest that better overall confinement than in the absence of ripple can probably be obtained at the expense of getting more violent ELMs by carefully choosing a suitable ripple amplitude profile. Above all, the study shows that ripple losses of thermal ions seem to be a highly important mechanism influencing the performance of tokamak plasmas in different and often counter-intuitive ways. These results may have profound implications for the design of future tokamaks and in particular for ITER, which is planned to operate with an intermediate level of toroidal magnetic field ripple and for which large divertor heat loads are a concern.

Acknowledgment: This work, supported by the European Communities under the contract of Association between EURATOM/Tekes, was carried out within the framework of the European Fusion Development Agreement. The views and opinions expressed herein do not necessarily reflect those of the European Commission.

[1] K. Tobita *et al.*, Phys. Rev. Lett. **69** 3060 (1992).
[2] G. Sadler *et al.*, Plasma Phys. Control. Fusion **34** 1971 (1992).
[3] G. Saibene *et al.*, Plasma Phys. Control. Fusion **46** A195 (2004).
[4] T. Kurki-Suonio *et al.*, Nucl. Fusion **42** 725 (2002).
[5] J. Lönnroth *et al.*, Plasma Phys. Control. Fusion **46** 767 (2004).
[6] B. Tubbing, Proc. 22nd EPS Conference on Plasma Physics and Controlled Fusion (1995).
[7] T. Kiviniemi *et al.*, Proc. 32nd EPS Conference on Plasma Physics (2005).
[8] P. Yushmanov, Review of Plasma Physics, v. 16, New York, Consultants Bureau (1990).